horticulturae

MDPI

Article

The Expression and Sequence Analysis of MdMATE52 in Apple Roots During Activation of Defense Against *Pythium ultimum* Infection

Yanmin Zhu [1,*], Bianca Ortiz-Uriarte [1], Jordan Rainbow [1] and Zhe Zhou [2,*]

[1] Tree Fruit Research Laboratory, Agricultural Research Service, United States Department of Agriculture, Wenatchee, WA 98801, USA; bianca.ortizuriarte@usda.gov (B.O.-U.); jordan.rainbow@usda.gov (J.R.)
[2] Zhengzhou Fruit Research Institute, Chinese Academy of Agricultural Sciences, Zhengzhou 450000, China
* Correspondence: yanmin.zhu@usda.gov (Y.Z.); zhouzhe@caas.cn (Z.Z.)

Abstract: To understand the molecular regulation of host defense responses in the pathosystem between apple roots and a necrotrophic oomycete pathogen *Pythium ultimum*, a series of transcriptome analyses have revealed a multi-phase and multi-layer defense tactic in apple root tissues. Among the most notable transcriptome changes during defense activation in apple roots, upregulation of genes involved in phenylpropanoid biosynthesis, transport of secondary metabolites, and lignin formation appeared to be the key defense themes which may crucially impact the outcome of plant–pathogen interactions. From our transcriptome datasets, the MdMATE52 gene, which encodes a MATE transporter, was shown to be differentially expressed between a resistant and a susceptible apple rootstock genotype in response to *P. ultimum* infection. The cis elements at promoter regions and sequence variations within coding regions of MdMATE52 were compared among several resistant and susceptible apple rootstock genotypes as well as various *Malus* species. The stronger upregulated expression patterns of MdMATE52 appeared to be correlated with the observed resistance traits among various genotypes. Our results suggested that minimal but clearly identifiable sequence variations may contribute to the genotype-specific expression and function of MdMATE52. The findings from this study should facilitate future experiments such as site-specific mutation and Crispr-based genome editing to define the regulation mechanisms of MdMATE52 and function during defense activation in apple roots.

Keywords: apple root; defense response; resistance trait; transporter; *Pythium ultimum*

check for updates

Citation: Zhu, Y.; Ortiz-Uriarte, B.; Rainbow, J.; Zhou, Z. The Expression and Sequence Analysis of MdMATE52 in Apple Roots During Activation of Defense Against *Pythium ultimum* Infection. *Horticulturae* **2024**, *10*, 1204. https://doi.org/10.3390/horticulturae10111204

Academic Editor: Yuepeng Han

Received: 27 September 2024
Revised: 31 October 2024
Accepted: 8 November 2024
Published: 15 November 2024

Copyright: © 2024 by the authors. Licensee MDPI, Basel, Switzerland. This article is an open access article distributed under the terms and conditions of the Creative Commons Attribution (CC BY) license (https://creativecommons.org/licenses/by/4.0/).

1. Introduction

Apple (*Malus* × *domestica* Borkh.) is one of the most popular tree fruits in temperate regions around the world [1]. The 2021 apple crop was valued at nearly USD 3.2 billion, grown on 382,000 acres of land in the United States (www.USAPPLE.org/, accessed on 10 September 2024). Every state including Michigan, New York, Pennsylvania, California, and Virginia in the United States grows apples, and 29 states grow apples commercially. Washington State produces approximately 60 percent of all US apples. Apple replant disease (ARD) threatens the survival of newly planted trees at a replant site, where apple or closely related tree species have been previously cultivated. The causal agents of ARD consist of a pathogen complex including necrotrophic soilborne oomycetes (*Phytophthora* and *Pythium*) and fungi (*Ilyonectria* and *Rhizoctonia*) [2,3]. Among them, *Pythium ultimum* is known to be one of the primary members in this pathogen complex and has been identified in orchard soils worldwide. Traditional management of ARD has almost exclusively depended on pre-plant fumigation of orchard soils to eradicate ARD pathogens, which is under increasing regulatory restriction due to environmental and human health concerns. Furthermore, the use of these chemical fumigants inadvertently eliminates beneficial soil

microbiota. The development and deployment of resistant apple rootstocks may offer a cost-effective, environment friendly and durable strategy for ARD management. Understanding the molecular regulation controlling defense activation in apple roots is a prerequisite for maximized exploitation of host resistance traits [4,5].

The defense responses of plants to pathogen infection are essentially chemical warfare due to their sessile nature. It is well established that a wide variety of secondary metabolites with extreme structural diversity are produced under stress conditions [6,7]. These compounds have multiple functions as protectants against UV light damage, oxidative stress, and pathogen attack. The most common groups of secondary metabolites include phenols, terpenoids, and alkaloids [8–10]. Most of these compounds are small molecules and their effective doses can be as low as 10^{-5}–10^{-4} M [6,7,11]. Both preformed antimicrobial compounds (phytoanticipins) and infection-induced antimicrobial metabolites (phytoalexins) are known to be associated with plant resistance to fungal, oomycete, and bacterial pathogens [6,11]. Phenolic compounds from the phenylpropanoid pathway are well documented to be associated with plant defense responses. Due to the potential cellular toxicity from these antimicrobial compounds, their biosynthesis is tightly regulated with specific temporal and spatial patterns. Therefore, the inherent capability of production of specific metabolites at proper timing and rates, and efficient transportation to the infection sites upon pathogenic challenge, can crucially determine the outcome of plant–pathogen interactions [12,13].

To understand the genotype-specific molecular regulation of defense responses to infection by *P. ultimum* in apple roots, a systematic phenotyping effort and three consecutive transcriptome analyses were carried out recently, including comparative transcriptomics and microRNA profiling as well as degradome sequencing [5,14–19]. Analyses of the comprehensive datasets have generated a high-resolution picture of the genome-wide transcriptional regulation between genotypes and during the infection process [5,14,17,18,20]. One of the primary regulation schemes associated with effective defense activation involves the swift upregulation of phenylpropanoid biosynthesis, robust transportation of secondary metabolites, and enhanced lignin deposition in infected tissues. Among the identified DEGs between resistant and susceptible apple rootstock genotypes, several gene families including those encoding MATE (Multidrug and Toxic Compound Extrusion) transporters were specifically responsive to *P. ultimum* infection, suggesting their potential contribution to apple root's resistance to infection by this pathogen [5,14,17,18,21].

Genes encoding MATE transporters belong to a well-conserved family that exists from microorganisms to plants and humans [22]. However, the members of this family appear to have vastly expanded in plant genomes, possibly due to the abundance of specialized metabolites in plant species. MATE proteins typically have 400–550 amino acid residues encompassing 12 transmembrane domains (TMDs). MATE transporters utilize an electrochemical gradient of either Na^+ or H^+ across the localized membrane as the driving force, and export primary and secondary metabolites from the cytoplasm to apoplasts or vacuoles. In plants, MATE transporters have been shown to be directly or indirectly involved in the processes of detoxification of noxious compounds or heavy metals, tolerance to aluminum toxicity, and disease resistance, and participate in transporting diverse types of secondary metabolites and hormones, such as ABA, salicylic acid, and auxin [22,23]. In the apple genome, a total of 66 MATE genes have been identified, indicating their wide-ranging biological functions [24].

In this study, the expression patterns of the apple MATE gene family were profiled in root tissues during the activation of defense against *P. ultimum* infection, and MdMATE52 was identified as a primary candidate for further examination. Its detailed sequence features, including coding and promoter regions, and genotype-specific expression were examined between O3R5 genotypes, i.e., the progeny from a cross population between 'Ottawa 3′ and 'Robusta 5′. The findings from this study may serve as a stepping stone for further investigation to understand the regulation of MdMATE52 expression and potential contribution to disease resistance in apple roots.

2. Materials and Methods

2.1. Apple Plant Micropropagation by Tissue Culture-Based Procedure

The apple plants used in this study were produced using a tissue culture-based micropropagation process as described in [15]. Briefly, four-week-old apple plants were prepared by micropropagation for infection assays. Prior to pathogen inoculation, these apple plants were transplanted from tissue culture medium to soils for one week of in-soil acclimation, which allows root tissue to further differentiate under soil conditions. Apple rootstock genotypes used in this study are members of the so-called O3R5 population (progeny from a cross between 'Ottawa 3' and 'Robusta 5') including the resistant genotypes O3R5-161, O3R5-58, and O3R5-78, and susceptible genotypes O3R5-106, O3R5-115, and O3R5-132 [16]. The legacy commercial cultivar Bud 9 (B.9) was also included. The genotype G.935 is a commercialized selection from the O3R5 population for its overall field performance in disease tolerance. For either pathogen-inoculated treatment or mock inoculation as controls, individual plants with similar ages and similarly sized root systems were randomly assigned to either group [17].

2.2. Inoculum Preparation, Inoculation by Root-Dipping, and Root Tissue Collection

Inoculum of *P. ultimum* was prepared with approximately 2×10^3 CFU (colony forming units) in 1% methyl cellulose solution as previously described [25]. The inoculation was performed by dipping the root system into the *P. ultimum* inoculum solution for 5 s. Control plants were mock-inoculated with 1% methyl cellulose solution. The treated plants were transplanted into pasteurized soil medium consisting of construction sands, perlite, and vermiculite in a 1:1:1 ratio. All plants were maintained in an environmental growth room at 23 °C ± 2 and under a 12/12 h light/dark photoperiod. Plant root tissues were harvested at 0, 24, 48, and 72 h post-inoculation (hpi). Root tissues were collected by excavating them from soil, washing them under tap water, and flash-freezing them in liquid nitrogen. Root tissues of 5 plants were collected and pooled as biological replicates at each timepoint per treatment.

2.3. RNA Isolation, cDNA Synthesis, Sequence Retrieval, Primer Design, and RT-qPCR

Total RNA isolation was performed as previously described [25]. The nucleotide sequences of selected candidate genes were downloaded from the Genome Database for Rosaceae (GDR, http://www.rosaceae.org/, accessed on 10 September 2024). Primers were designed using Primer3Plus (https://www.primer3plus.com/, accessed on 10 September 2024) with the following criteria: GC content 45–65%, Tm > 50 °C, primer length 20–24 bp, and amplicon size 150–200 bp (Table 1). Total RNA was quantified using an ND 1000 Nanodrop spectrophotometer (NanoDrop Technologies, Wilmington, DE, USA) and the RNA quality was verified by agarose gel electrophoresis. Total RNA was treated with DNase I (Qiagen, Valencia, CA, USA) and then purified with RNeasy cleanup columns (Qiagen, Valencia, CA, USA). One microgram of DNase-treated RNA was used to synthesize first-strand cDNA using SuperScriptTM II reverse transcriptase (Invitrogen, Grand Island, NY, USA) and poly dT (Operon, Huntsville, AL, USA) as the primer. The cDNA was diluted 20 times and a 4 µL aliquot was used in a 20 µL quantitative PCR (qPCR) reaction mix: 10.0 µL iTaq Universal SYBR Green Supermix (Biorad, Hercules, CA, USA), and 0.4 µM forward/reverse primer (IDT, Coralville, IA, USA). RT-qPCR was performed in 96-well plates by using a CFX real-time qPCR detection system (Biorad Lab, Hercules, CA, USA) and the following protocol: cycle conditions of 3 s at 95 °C and 40 cycles of 10 s at 95 °C and 30 s at 60 °C. The melting curve for each amplicon was obtained from 60 to 95 °C to verify primer specificity. The PCR efficiency and correlation coefficient (R^2) for each primer set were calculated by the slopes of standard curves generated in Microsoft Excel 365 from a 10-fold cDNA dilution series (1:1, 1:10, 1:100, 1:1000, and 1:10,000). All assays were carried out in two technical and biological replicates with template-free negative controls being performed in parallel. The target gene expression was normalized to that of a previously validated internal reference gene (MDP0000095375) specific for gene expression analysis in apple roots using the $2^{-\Delta\Delta CT}$ method (the comparative Ct method) [26]. The reported values represent the

average fold changes between control and treated samples with SD from the raw values of these assays based on *t*-tests.

2.4. RNA-Seq-Based Transcriptome Analysis of Defense Response in Apple Roots per Genotype and Timepoint

Total RNA isolation and high-throughput mRNA sequencing followed the methods previously described [25]. Root tissues of both resistant G.935 and susceptible B.9 were represented by three biological replicates, and each replicate included the pooled root tissues from five plants. Four timepoints were set, i.e., 0, 24, 48, and 72 hpi. The frozen root tissue samples were ground to a fine powder in liquid nitrogen, and RNA quantity was determined using a Nanodrop spectrophotometer. The RNA integrity number (RIN) was evaluated using an Agilent 2100 Bioanalyzer. Only RNA with an RIN value of $x \geq 8$ was used for RNA-Seq. The library preparation and RNA sequencing with 150 bp paired-end (PE) reads were completed at the Center for Genome Research and Biocomputing at Oregon State University using an Illumina HiSeq™ 3000 (Illumina Inc., San Diego, CA, USA). The original RNA-seq data were deposited in the SRA (Sequence Read Archive) at the NCBI website under the accession number SRP117760 (ftp://ftp-trace.ncbi.nlm.nih.gov/sra/review/SRP117760, accessed on 10 September 2024). Reads from B.9 and G.935 libraries were mapped to the nucleotide sequences of predicted coding genes of the *Malus* × *domestica* Whole Genome v3.0.a1 (https://www.rosaceae.org/analysis/162, accessed on 10 September 2024) using the ultrafast, memory-efficient short read aligner Bowtie2-2.2.5 which utilizes a Burrows–Wheeler index [27]. Count data were obtained for each and all predicted coding sequences. Raw counts for each gene were normalized using the DESeq2 package [28] and R x64 3.3.1 program (http://www.r-project.org/, accessed on 10 September 2024). Differentially expressed genes (DEGs) were identified by comparing transcript abundance between mock-inoculated control root tissues and those from *P. ultimum*-infected root tissues with the cutoff values of Log_2Fold Change ≥ 1 and the padj (adjusted *p*) values ≤ 0.05. The annotation of these genes was carried out by BLASTP [29] against the NR (non-redundant protein sequences) database, and a BLAST database containing genomic sequences for Arabidopsis (*Arabidopsis thaliana*), corn (*Zea mays*), *Medicago truncatula*, rice (*Oryza sativa*), and tomato (*Solanum lycopersicum*). A heatmap illustrating the expression of the 66 identified MATE genes was generated in R using the pretty heatmap package: *pheatmap* [30].

2.5. Cloning of Genomic Copy of MdMATE52 from Selected Apple Rootstock Genotypes and Sequence Retrieval from GDR for Selected Malus Species

PCR primers, for amplification of both 2 kb promoter regions and 5′-coding regions (Table 1), were designed based on the retrieved sequences from the public domain (GDR—Genomic Database for Rosaceae, https://www.rosaceae.org, accessed on 10 September 2024). The genomic DNAs from these apple rootstock genotypes, including those from the O3R5 cross population and a commercial apple rootstock cultivar B.9, were isolated from leaf tissues using the DNeasy Plant Pro Kit (Qiagen, Valencia CA, USA) for amplifying and cloning of designated regions. PCR amplification was carried out using a Techne TC-512 (GMI, Ramsey, MN, USA). For sequence determination, at least five independent positive colonies were cloned using the NEB® PCR Cloning Kit (NEB #E1202S, Ipswich, MA, USA), and the three inserts were sequenced at Molecular Cloning Lab (https://mclab.com/, accessed on 10 September 2024). Promoter sequences for MdMATE52 homologs from several species including *M. domestica* (HFTH, GDDH), *M. baccata*, *M. prunifolia*, and *M. sylvestris* were retrieved from GDR. The primer sequences for cloning genomic fragments for MdMATE52, as well as those used for RT-qPCR, are listed in Table 1.

Table 1. Primer sequences for amplifying genomic fragments and qRT-PCR reaction.

Gene # Functional Annotation	Primer F/R [5′-3′]
MD14G1012300 MATE52 promoter region Set 1	F-5′ AAGTTCGTATCCGCAATGGC 3′
	R-5′ TGTTCCGAATGACGCAACTC 3′
MATE52 promoter region Set 2	F-5′ GTCCGAATTGCGTCAACTTCC 3′
	R-5′ ACTAAGGTTTGCGTTCCCACA 3′
Coding region	F-5′ TTGGCATGGCAAGTGCGC 3′
	R-5′ TGGAAACAGTACCGGAGAGCA 3′
qPCR	F-5′ CATCGTGGGGTGGGAAATGA 3′
	R-5′ CGCCTTTGAGCTACCTCCTC 3′
MD02G1221400 Reference gene	F-5′ ACATCGAGAGCTTTGGCTAAC 3′
	R-5′ CTCCATCAGAACCACTGACATC 3′

2.6. Bioinformatic Analysis for the Selected Sequences of MATE Genes per Genotype and Malus Species

The services on the PlantCARE [31] (https://bioinformatics.psb.ugent.be/webtools/plantcare/html/, accessed on 10 September 2024) and PlantPAN [32] (https://plantpan.itps.ncku.edu.tw/, accessed on 10 September 2024) websites were used to generate the predicted binding sites for various transcription factors. The outputs from these online analytical tools were combined to balance conciseness and coverage. The categories and distribution of predicted cis elements or binding sites for major transcription factors or hormone responses may provide the hints about the roles of these factors in plant defense responses to biotic stress. These cis elements are well established for their potential roles in plant defense activation and phenylpropanoid pathway biosynthesis. SMART (http://smart.embl-heidelberg.de/, accessed on 10 September 2024) was used to identify the conserved transmembrane domains and other possible signal peptides. Line figures were generated using TBtools software [33]. The original gene names in our transcriptome dataset reflect the nomenclature of the only *Malus domestica* genome of 'Golden Delicious' available at that time [34]. Two other apple genome sequences, GDDH13 [35] and HFTH [36], later became available, offering better coverage and greater accuracy, but used different gene naming schemes than the first genome. Our bioinformatic analyses used the BLAST+ function in GDR to convert between gene names from different apple genome versions. This procedure required judgment of the best gene match by balancing both the length and degree of sequence similarity between gene IDs. For 10 of the 66 apple MATE genes from the article on the apple MATE family [24], the best aligned gene ID from our transcriptome data was shared with another MATE gene. This discrepancy is likely due to the level of coverage for the genome, difference in plant materials, and improvement in sequencing technology as well as better assembling tools. For example, MdMATE11 and MdMATE23 best aligned to MDP0000226135, and MdMATE46, MdMATE59, MdMATE60, and MdMATE61 are best matched to MDP0000310842 in the resulted heatmap. Similarly, the best-matched gene ID for MdMATE47 and MdMATE48 is MDP0000277246, and for MdMATE50 and MdMATE62, the best match is MDP0000313254.

3. Results

3.1. Distinct Resistance Responses Between O3R5 Apple Rootstock Genotypes to P. ultimum Infection

From a recent systematic phenotyping effort, distinct resistance responses to inoculation with a soilborne necrotrophic oomycete pathogen *P. ultimum* have been identified among O3R5 apple rootstock genotypes and other legacy rootstock cultivars. As illustrated in Figure 1A, using our standardized phenotyping protocol, a wide range of resistance responses such as plant survival rates have been repeatedly observed for a specific genotype. The plant survival rates at 14 dpi (days post-inoculation) varied from lower than 30% for those designated as susceptible genotypes to over 80% for those designated as resistant genotypes [5,15,16]. Figure 1A demonstrates three representative levels based on plant survival rates, i.e., highly susceptible (left), mediocre (middle), and highly resistant (right) in response to *P. ultimum* inoculation. Under the microscope, contrasting features of tissue necrosis progression between resistant and susceptible genotypes can often be observed along infected root branches (Figure 1B–D). Figure 1B shows, as a mock inoculation control, intact root tissues with typical white color without detectable discoloration at 48 hpi (hours post-inoculation). The pathogen-inoculated root tissues from resistant genotypes often exhibited a feature of sudden stoppage of necrosis progression, resulting in a clear separation between healthy and necrotic sections of tissues (red arrows in Figure 1C), which suggests that an effective defense mechanism exists. On the other hand, pathogen-inoculated susceptible genotypes commonly showed quick and widespread tissue collapse along the infected root branches, typically with brown to yellow coloration as well as profuse growth of pathogen hyphae (red arrows in Figure 1D), which indicates a compromised defense response to *P. ultimum* inoculation. These genotypes with consistent resistance phenotypes provided crucial plant materials for investigating the molecular controls underlying apple root pathogen resistance.

3.2. Expression Profile of the MATE Gene Family in Response to P. ultimum Infection Between Resistant and Susceptible Genotypes

A comprehensive dataset of RNA-seq-based transcriptome analyses on defense responses in apple roots [17] makes it possible to profile the expression patterns for each of the 66 members in the apple MATE gene family [24]. Using average values of transcript counts from three independent biological replicates per sample, Figure 2 summarizes the expression intensity for every apple MATE gene between the resistant genotype G.935 and the susceptible genotype B.9 at three timepoints of 24, 48, and 72 hpi. As represented by color shades in the heatmap (Figure 2), about one-third of gene family members, i.e., up to 22 of them, showed no expression or very low expression (as indicated by dark to light blue) in apple root tissues. A moderate level of expression (yellow to light orange) can be detected for approximately another one-third of the genes. About 16–17 MATE genes, slightly over a quarter of the entire gene family, showed a relatively higher expression level as indicated by darker orange to red colors.

With few exceptions, most MATE gene family members showed no identifiable variation in expression levels between mock-inoculated and pathogen-infected tissues, suggesting that those genes were not directly involved in defense activation in apple roots to *P. ultimum* infection. Among those genes exhibiting noticeable upregulation in pathogen-infected samples as compared to the corresponding mock inoculation controls (arrows), most of them exhibited an inconsistent induction or irregular changes in expression levels. Noticeably, MdMATE52 showed a rather consistent upregulation at all timepoints in response to pathogen infection. Perhaps more importantly, its upregulation appeared to be differential between resistant G.935 and susceptible B.9. Specifically, MdMATE52 demonstrated an earlier and stronger induction in the roots of resistant G.935 than in the roots of susceptible B.9. Therefore, MdMATE52 was selected as a target candidate gene for additional analysis.

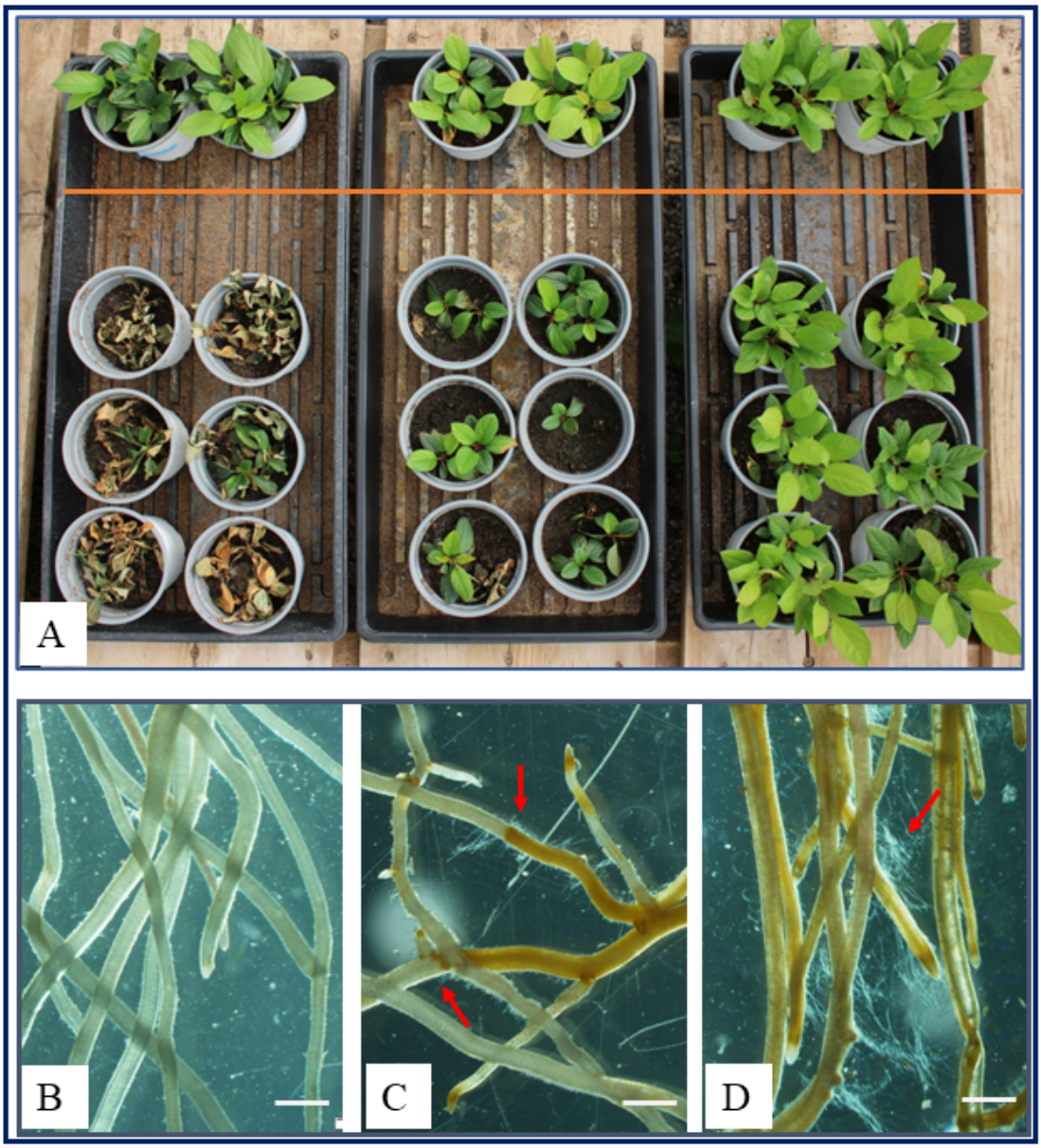

Figure 1. Representative images exhibiting various resistance responses among O3R5 genotypes in the form of plant survival rates and progression patterns of tissue necrosis. Using a single inoculum preparation in one infection assay, widely variable plant survival rates were observed at 14 dpi among genotypes. (**A**) Susceptible line O3R5-106 (**left**), mediocre line O3R5-80 (**middle**), and resistant line O3R5-78 (**right**). The plants in the pot on the top row in each tray were the mock inoculation controls for each genotype; *P. ultimum*-inoculated plants were in a group of 6 pots (three plants per pot), shown below the orange-colored line. (**B**) A representative image of mock-inoculated apple roots under a dissection microscope, showing intact root tissues with typical white color at 48 hpi without any detectable discoloration. (**C**) A representative microscopic image showing stopped or disrupted necrosis progression in *P. ultimum*-inoculated apple roots of a resistant O3R5 genotype at 48 hpi, as indicated by the presence of clear-cut "boundaries" or "lines" (red arrows) separating healthy and necrotic sections with minimal pathogen hyphae visible. (**D**) A representative image showing widespread tissue necrosis with collapsed root tissues and yellow-brownish coloration, and profuse growth of pathogen hyphae (red arrow) in the roots of a susceptible genotype at 48 hpi. The bars represent 500 μM in length.

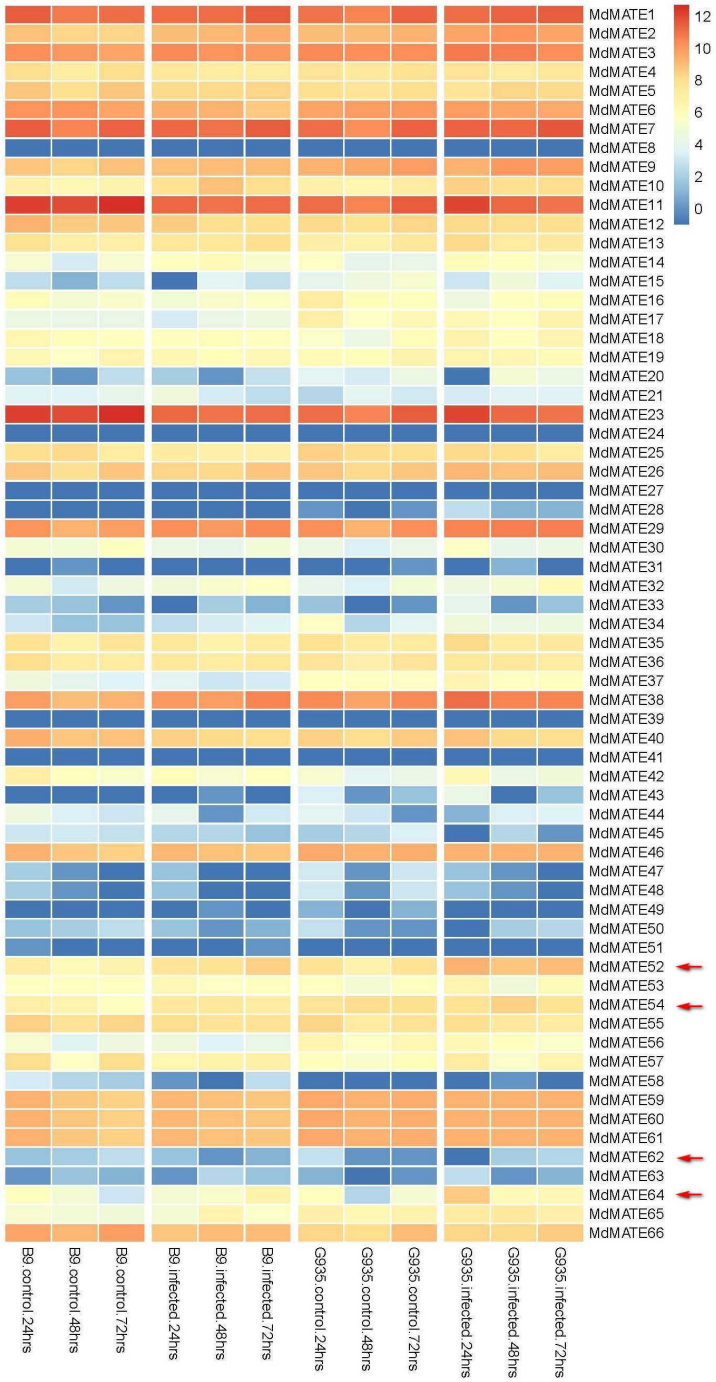

Figure 2. The expression profile of the apple MATE gene family in apple roots at three timepoints after *P. ultimum* inoculation between a resistant G.935 and a susceptible B.9 genotype. The heatmap summarizes the expression level and dynamic change during infection for each apple MATE gene based on normalized values (among the entire sample set) of transcript counts from the RNA-seq-based transcriptome dataset. The detected values are in the range of 0–10^6. Because of the discrepancies of gene models between two genome sequences, e.g., improved sequencing technology and refined germplasm (double or triple haploids) used to obtain the newer apple genome sequences, occasionally, several gene models from GDDH match the same gene model from our transcriptome data (for example, MdMATE59, MdMATE60, and MdMATE61). Red arrows indicate those genes exhibiting noticeable upregulation in pathogen-infected samples as compared to the corresponding mock inoculation controls.

3.3. Basic Bioinformatics About the MdMATE52 Gene

The sequence of MdMATE52 indicates that it encodes a typical plant MATE transporter as described below. Using the HFTH genome sequence as a reference, the full-length transcript of MdMATE52 consists of 3081 bp, with a coding region of 1485 bp, which translates to 494 amino acid residues. As shown in Figure 3A, the predicted gene structure of MdMATE52 contains eight exons and seven introns, which is common to the MATE gene structure in other plant species and some apple MATE genes. The SMART analysis of amino acid sequences predicts 12 transmembrane domains, which is a standard feature across the MATE proteins (Figure 3B). MdMATE52 is located on the top end of chromosome 14 (Figure 3C). It should be noted that our transcriptome data were analyzed using the then-available apple genome sequences (v3.01). In the current study, to align with a reported naming system of apple MATE gene family members [24], the original gene IDs from our transcriptome data were converted to IDs from the newer version of apple genome sequences. The corresponding gene names for MdMATE52 in three commonly referenced genome sequences are MDP0000161125 (in first apple genome sequences of 'Golden Delicious'), MD14G1012300 (in GDDH13), and HF19931 (in HFTH).

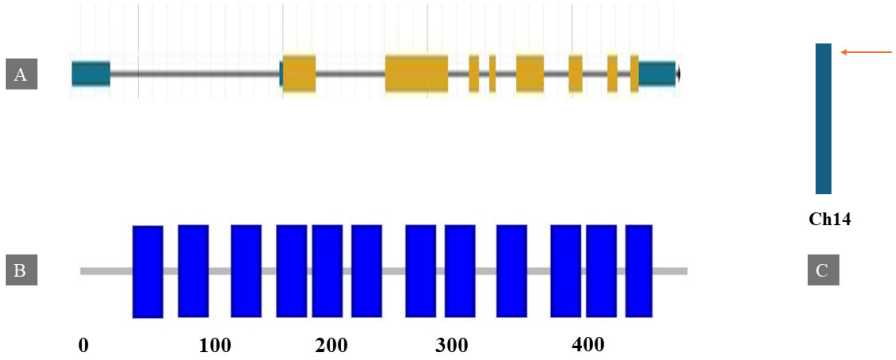

Figure 3. Basic sequence features and gene structure of MdMATE52. (**A**) Predicted introns, exons (yellow bars), and untranslated regions (green bars). (**B**) Predicted 12 transmembrane domains (blue bars) from the amino acid sequences from the SMART domain prediction. (**C**) The genomic location on the tip of chromosome 14 (red arrow).

3.4. Variations in Predicted Cis Elements in the Promoter Region of MdMATE52 Among O3R5 Genotypes and Malus Species

The sequence variations at the 5′ flanking region of the MdMATE52 gene, or its promoter region, may contain information for explaining regulatory features of its expression during interaction with *P. ultimum*. A total of 2 kb of the promoter region from each of four O3R5 genotypes (two resistant and two susceptible ones) was cloned, sequenced, and subjected to bioinformatics analysis. Figure 4 summarizes the distribution of predicted binding sites for selected major transcription factors and/or hormone pathways relevant to plant biotic stress response. As shown in Figure 4A, most cis elements are largely shared across O3R5 genotypes as expected, yet minor but identifiable variations were detected between genotypes such as slight shifts of position for specific binding sites. In general, the cis elements related to hormone responses are the same across these genotypes. On the other hand, binding sites for four out of five transcription factor families showed noticeable differences. An NAC (transcription factor family including three subgroups of NAM, ATAF, and CUC) binding site is absent from G.935 at the proximal end near the -100 bp position; at the same time, an extra NAC binding site is located at the distal end of the promoter region for the susceptible B.9. In total, two extra NAC binding sites are present in the B.9 promoter in comparison to that of G.935. The noticeable variations between B.9 and O3R5 genotypes are probably less surprising as B.9 does not share a similar genetic background to O3R5 genotypes. Also, between B.9 and G.935, an extra bHLH (basic helix–loop–helix) binding site was detected at −380 bp and an extra MYB (myeloblastosis-related protein) binding

site at −1100 bp only in G.935 but not B.9. Additionally, a TCP binding site is missing at the distal part of the B.9 promoter, compared to all O3R5 genotypes. The biological context of binding site presence and locations could be an interesting subject for future study.

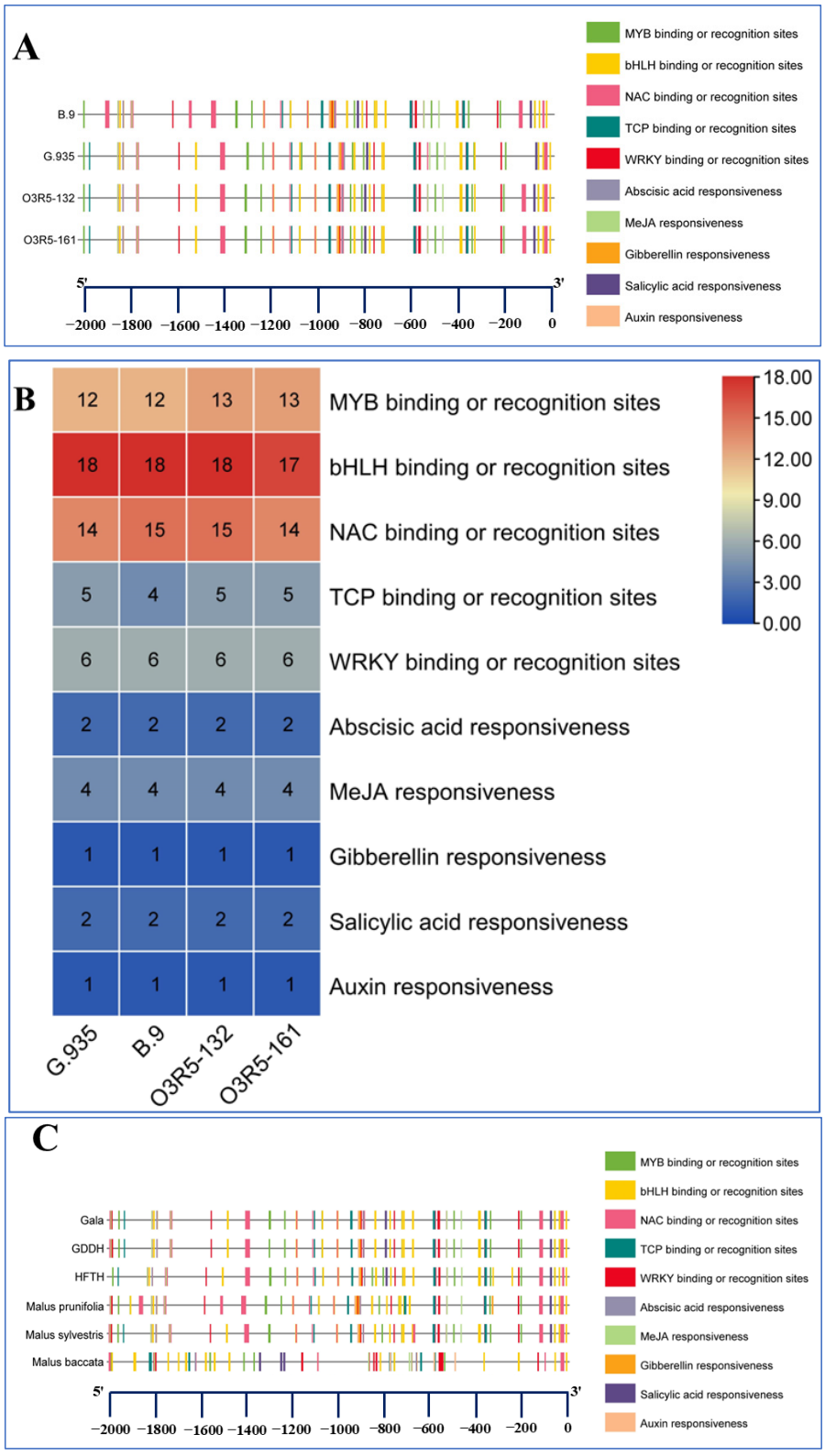

Figure 4. *Cont.*

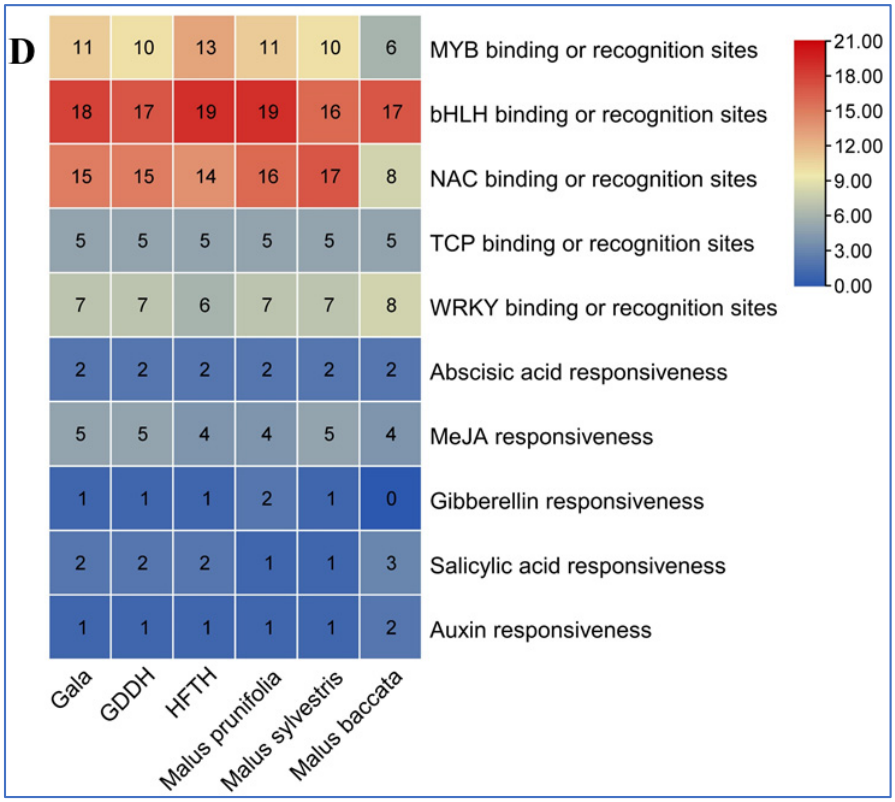

Figure 4. Predicted cis elements within the 2 kb promoter region of the MdMATE52 gene among O3R5 genotypes and several *Malus* species. (**A**) The position and distribution patterns of predicted cis elements for three O3R5 genotypes and B.9. (**B**) Heatmap representing the numbers of putative cis elements by categories for three O3R5 genotypes and B.9. (**C**) The position and distribution patterns of predicted cis elements for multiple *Malus* species. (**D**) Heatmap representing the numbers of putative cis elements by categories for multiple *Malus* species. The thickness of the vertical lines reflects the length of the core binding site. Occasionally overlapped or juxtaposed sites at the same locations make the clear separation of tightly neighboring binding sites difficult; the exact numbers of each category of binding site are expressed in the heatmap.

Furthermore, retrieved promoter sequences for MdMATE52 homologous genes from several *Malus* species, including several wild apples (where O3R5 genotypes originated), were similarly analyzed. As shown in Figure 4B, the cis elements for MdMATE52 genes from these species demonstrated largely comparable patterns of predicted transcription factor (TF) binding sites. One obvious exception is *M. baccata*, in which the promoter region exhibits remarkable variations from cultivated apples and other *Malus* species for several categories of cis elements. For example, at the proximal end of the 2 kb promoter sequences of *M. baccata*, several MYB, bHLH, and NAC binding sites are absent, but an extra NAC binding site was detected near the distal part compared to other *Malus* species. Also, an extra auxin responsiveness element is present at the -500 bp position. While three cultivated apple cultivars showed two elements related to salicylic responsiveness near the proximal end and another one at the middle section of the promoter, a cluster of three of them were detected near the distal section (−1300 bp position) of the 2 kb promoter region of *M. baccata*. On the other hand, two other wild apple species only displayed one salicylic responsiveness binding site at the proximal position, similar to the cultivated apples. The distribution pattern for three out of five TCP binding sites in *M. baccata* were shifted in the distal direction compared to other species. In addition to one extra WRKY binding site detected, two other WRKY (TF-containing conserved amino acid sequence WRKYGQK at its N-terminal end) binding sites were shifted in the distal direction, which is specific to the promoter of *M. baccata* but not to the rest of the species. Moreover, one extra

salicylic responsiveness binding site was detected and a total three of them were clustered together in the middle part of the 2 kb sequences, which is unique to this species.

3.5. Detected Sequence Variation Within Coding Sequences

We cloned and sequenced an approximately 1.5 kb region of the MdMATE52 gene from six O3R5 genotypes (three resistant genotypes: O3R5-58, O3R5-161, G.935; and three susceptible genotypes: O3R5-47, O3R5-115, O3R5-132). The reference sequence of MdMATE52 was taken from HFTH, a tri-haploid originating from a cultivar named HanFu, which is a recently released high-quality apple genome sequence and has a relatively closer genetic background with O3R5 genotypes. Using HFTH sequences as a reference, the six O3R5 genotypes showed variation at an aggregate of 10 nucleotides, although their positions were variable between genotypes (Table 2). Four of these variations, including one insertion, occurred in intron regions, while six of them occurred in exons. Three mutations of those in exons lead to amino acid codon change, but no conversions leading to termination codon were detected. Between resistant and susceptible genotypes, no consensus of mutations was observed. Only two mutations at nucleotide positions 41 and 786, both in exons, were shared across all O3R5 genotypes. Therefore, because of the lack of consensus of mutation, it is less likely that these identified sequence variations between two groups of O3R5 genotypes can be attributed to the observed resistant traits. Nevertheless, these verified nucleotide sequences in each genotype are pivotal for designing guide sequences for CRISPR-Cas9-based genome editing in future transgenic studies using these O3R5 genotypes as starting plant materials.

Table 2. Variation in nucleotide sequences within the coding region among six O3R5 genotypes.

HF Reference Position	58 R	161 R	G935 R	47 S	115 S	132 S	Intron or Exon	Codon Change	Amino Acid Change
41	A > G	A > G	A > G	A > G	A > G	A > G	Exon	TCA > TCG	None
42		T > C		T > C		T > C	Exon	TAT > CAT	Y > H
296		G > A	G > A	G > A		G > A	Exon	GCG > GCA	None
364		A > T	A > T	A > T		A > T	Exon	TAT > TTT	Y > F
614/615		G INS	G INS	A INS	G INS	G INS	Intron	NA	NA
630		C > T	C > T	C > T		C > T	Intron	NA	NA
786	G > T	G > T	G > T	G > T	G > T	G > T	Exon	GTG > GTT	None
885			G > T		G > T		Intron	NA	NA
995		G > A	G > A	G > A		G > A	Intron	NA	NA
1164	G > A						Exon	GGA > AGA	G > R

The coding sequences of MdMATE52 for six O3R5 genotypes were determined by cloning and sequencing the 5′ one-third of the genomic sequences. The sequences for individual genotypes were determined using three independent plasmids and from both directions of the insert to minimize introduced error from sequencing itself. Intron/exon junctions were manually assigned based on the HF19931 reference sequence. The amplified region was designed to skip the first long intron and start at the beginning of the second long exon, covering the end of the fourth exon. Primer sequences used for amplifying these fragments are listed in Table 1.

3.6. Expression Patterns of MdMATE52 During Defense Activation Among O3R5 Genotypes

Although RNA-seq-based transcriptome analysis indicated that MdMATE52 exhibited a differential expression pattern between genotypes G.935 and B.9, it remains interesting to cross-examine whether similar patterns can be observed using qRT-PCR and in other resistant and susceptible apple rootstock genotypes. As shown in Figure 5A,B, between G.935 and B.9, similar upregulation patterns to those observed from transcriptome data were demonstrated, i.e., a higher level of induction of MdMATE52 in the resistant G.935 compared to that in B.9. Probably more importantly, a similarly distinguishable expression pattern of MdMATE52 was also exhibited between another pair of O3R5 genotypes,

i.e., a resistant O3R5-78 and a susceptible O3R5-106. In the latter case, upon challenge by *P. ultimum*, a stronger and consistent upregulation of MdMATE52 expression was observed at all timepoints in the root of the resistant genotype O3R5-78; in contrast, a minimal and often inconsistent upregulation of its expression was observable in the susceptible O3R5-106 (Figure 5C,D). Although RNA sequencing and PCR amplification employ different biochemistry, the induction trends of the MdMATE52 gene between resistant and susceptible apple rootstock genotypes following *P. ultimum* infection are largely comparable. Therefore, in terms of MdMATE52 expression patterns, it appeared that the results from the large-scale high-throughput transcriptome dataset are basically transferable to other apple rootstock genotypes, in terms of their gene induction patterns, at least in this pathosystem between apple roots and the necrotrophic oomycete pathogen *P. ultimum*.

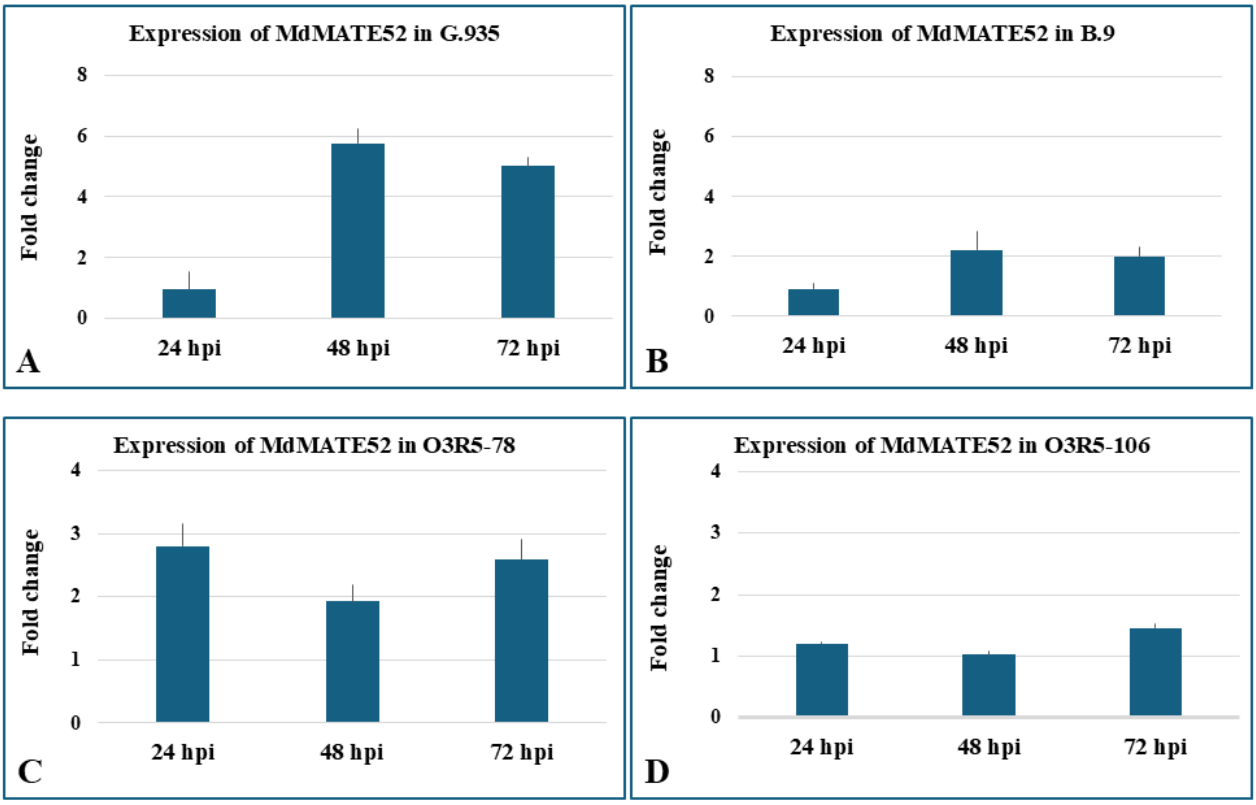

Figure 5. The upregulation patterns of MdMATE52 between resistant and susceptible genotypes during *P. ultimum* infection. (**A**) The upregulation pattern in the root tissues of a resistant genotype G.935. (**B**) The upregulation pattern in the root tissues of a susceptible genotype B.9. (**C**) The upregulation pattern in the root tissues of a resistant genotype O3R5-78. (**D**) The upregulation pattern in the root tissues of a susceptible genotype O3R5-106. The y-axis shows the fold change in gene expression, calculated as the ratio of detected values in *P. ultimum*-infected tissues over those in the mock inoculation control at the same timepoint. Detected values of relative expression level in the tissues right before the infection process, or a timepoint of 0 hpi, were used as a calibrator for each genotype.

4. Discussion

Elucidating the molecular regulation of resistance responses in apple roots to infection from the necrotrophic *P. ultimum* has been our research focus recently [4,14–18,25,37,38]. In the last few years, three consecutive transcriptome analyses and the resulting comprehensive datasets have allowed us to identify key candidate genes in specific pathways which are differentially expressed during defense activation between resistant and susceptible genotypes [14,17,18]. Among the most notable transcriptome changes are the consistent upregulation of genes functioning in the phenylpropanoid and flavonoid biosynthesis pathways, transportation of secondary metabolites, and laccase-directed lignin forma-

tion [14,17,18]. At the same time, a systematic phenotyping effort, among more than 90 O3R5 apple rootstock genotypes, has identified an elite panel of genotypes with contrasting resistance responses to *P. ultimum* infection [15,16,25]. Their phenotypic characterizations include genotype-specific plant survival rate and microscopic features of tissue necrosis progression, as well as anatomical, cellular, and biochemical alterations due to *P. ultimum* infection [39,40]. Progress in transcriptome analysis-based candidate gene discovery and the phenotyping of resistance traits makes it feasible to design experiments with the goal of associating specific candidate genes with defined resistance phenotypes. In this study, a closer examination of MdMATE52 was carried out using expression and sequence analyses to evaluate its potential connection to root resistance against invading *P. ultimum*.

Plant cells, similar to those of most other organisms, are capable of removing potential toxic compounds, including those produced endogenously such as phenolics, flavonoids, and phytoalexins, from the cytoplasm by either sequestering them in vacuoles or transporting them to the cell wall [41]. Plant MATE genes encode proteins that are believed to function as transporters of these secondary metabolites and phytohormones [22,42]. From our transcriptome analyses, multiple genes encoding MATE proteins are specifically responsive in apple roots during infection by *P. ultimum*. A careful examination of the expression profile of the apple MATE gene family uncovered that MdMATE52 was expressed differentially between a resistant genotype G.935 and a susceptible genotype B.9 upon challenge by *P. ultimum* infection. In other words, MdMATE52 exhibited an early and consistent upregulation in infected root tissues of a resistant genotype G.935. In contrast, a minimal and inconsistent upregulation was found in a susceptible genotype B.9. The contrasting expression profiles of MdMATE52 between these genotypes suggest its potentially crucial role for an efficient defense activation against *P. ultimum*.

Categories and positions of specific cis elements in the promoter region of MdMATE52 and their variations between genotypes can impact the gene's expression patterns and functional roles during plant–pathogen interactions. Plant growth, development, and defense are primarily coordinated by the activity of sequence-specific transcription factors (TFs), a class of proteins that regulate gene expression in response to internal cues and external signals. TFs typically have a modular structure, comprising a DNA-binding domain together with a transcriptional regulatory domain, and they can function as transcriptional activators, repressors, or both. Several families of TFs are well known to be the important regulators of plant defense response to biotic or abiotic stresses [43–45]. In apple roots, MYBs, NACs, and WRKY are among other families which are actively involved both transcriptionally and post-transcriptionally in response to *P. ultimum* infection [5,14,17,18]. MYB, as a super TF family, is particularly important for the phenylpropanoid pathway and is often paired with the bHLH binding sites [46,47]. The WRKY family is also well known for its roles during plant defense activation against necrotrophic pathogens [48–50]. In this study, minor but identifiable variations regarding the cis elements were identified within 2 kb promoter regions between resistant and susceptible O3R5 genotypes as well as B.9. Yet, more remarkable differences were observed between several *Malus* species. The molecular or biochemical nature of these observed variations in binding site distribution along the promoter region, or in vivo significance, is beyond the current study. Nevertheless, these findings regarding binding site variations deserve to be investigated in future studies for their potential effect on MATE gene expression and potential contribution to disease resistance.

The increased availability of apple genomic resources greatly enabled the current study. Currently at least six apple genome sequences are publicly available including those for wild apple germplasm, or *Malus* species, which are often used for apple rootstock breeding and those considered the progenitors of cultivated apple [34–36,51,52]. However, the genome sequences for O3R5 genotypes, the plant materials used in this study, are not currently available. In this study, the genomic copies of MdMATE52 from several resistant and susceptible O3R5 genotypes as well as B.9 were cloned, sequenced, and aligned to examine the genotype-specific variations at the nucleotide level. Between resistant

and susceptible genotypes, the sequence variations at both coding and promoter regions provided useful insight which may help to explain the divergent expression behaviors between genotypes during defense activation. For example, the presence or distribution patterns of cis elements at the MdMATE52 promoter regions could shed light on the involvement of internal cues and external factors in regulating the gene's expression. Furthermore, accurate nucleotide sequences within the coding region of MdMATE52 are essential requirements for designing the guide RNA for performing CRISPR-Cas9-based genome editing in subsequent transgenic gene-knockout studies. It should be noted that our transcriptome data were analyzed using the only available apple genome sequence of the commercial 'Golden Delicious' cultivar at the time [34]; however, two other apple genome sequences, GDDH13 [35] and HFTH [36], were released later with better quality and coverage of the genome due to using better defined plant materials and newer sequencing technology such as PacBio. For the section on the expression profiling of the MATE gene family, the original gene names from our transcriptome data were converted to those in the GDDH13 genome to match the naming system of apple MATE genes from a recent report [24]. For example, the gene ID of MdMATE52 corresponds to MDP0000161125 in our transcriptome data and was converted to MD14G1012300 in order to match the naming system of GDDH13. Similarly, for analysis of variation at the nucleotide level, HF19931 in the HFTH genome was used to replace MDP0000161125.

5. Conclusions

In summary, based on previous transcriptome analyses, our working hypothesis has been that resistance to *P. ultimum* infection in apple roots depends primarily on the speed and intensity at which antimicrobial phenolics, including lignin, are produced in infected tissues. Quick production and efficient transportation of lignin precursors, or monolignol subunits, and other antimicrobial phenolic metabolites could operate as one of the key regulatory nodes which may ultimately differentiate resistance from susceptibility. A panel of O3R5 apple rootstock genotypes with reliable resistance phenotypes from our phenotyping project provided essential materials to test this hypothesis by correlating the expression of individual genes to resistance performance following *P. ultimum* infection [4,5,19]. The role of laccase-directed lignin biosynthesis and resulting cell wall fortification in plant disease resistance has been proposed for several decades in different pathosystems [13,53]. Accumulating evidence indicates that the lignified cell wall serves as a physical barrier against invading phytopathogens as well as other environmental stresses [54–57]. However, in the pathosystem between apple roots and *P. ultimum*, the role of pathogen-induced lignification and its contribution to resistance have not been studied until recently [18,21]. In the current study, our findings expanded our understanding of the sequence features of MdMATE52 and its connection to apple root resistance traits. The molecular basis of how MdMATE52 influences the interaction between apple roots and *P. ultimum*, presumably as a transporter of monolignols, deserves a subsequent analysis by biochemical and transgenic approaches.

Author Contributions: Y.Z. conceived the scope of this review manuscript and wrote most of the manuscript. J.R. and B.O.-U. provided the raw data and were involved in writing. Z.Z. participated in writing and was involved in manuscript revision. All authors have read and agreed to the published version of the manuscript.

Funding: This work was supported by USDA ARS base fund.

Data Availability Statement: Data are contained within the article.

Conflicts of Interest: The authors declare no conflicts of interest regarding the publication of this paper.

References

1. Janick, J.; Cummins, J.; Brown, S.; Hemmat, M. Apples. *Fruit Breed.* **1996**, *1*, 508. [CrossRef]
2. Jaffee, B.; Abawi, G.; Mai, W. Fungi associated with roots of apple seedlings grown in soil from an apple replant site. *Plant Dis.* **1982**, *66*, 942–944. [CrossRef]
3. Mazzola, M. Elucidation of the microbial complex having a causal role in the development of apple replant disease in Washington. *Phytopathology* **1998**, *88*, 930–938. [CrossRef]
4. Zhu, Y.; Fazio, G.; Mazzola, M. Elucidating the molecular responses of apple rootstock resistant to ARD pathogens: Challenges and opportunities for development of genomics-assisted breeding tools. *Hort. Res.* **2014**, *1*, 14043. [CrossRef]
5. Zhu, Y.; Saltzgiver, M. A systematic analysis of apple root resistance traits to *Pythium ultimum* infection and the underpinned molecular regulations of defense activation. *Hort. Res.* **2020**, *7*, 62. [CrossRef]
6. Dixon, R.A. Natural products and plant disease resistance. *Nature* **2001**, *411*, 843. [CrossRef]
7. Grayer, R.J.; Kokubun, T. Plant–fungal interactions: The search for phytoalexins and other antifungal compounds from higher plants. *Phytochemistry* **2001**, *56*, 253–263. [CrossRef]
8. Geilfus, C.-M. Plant Secondary Compounds. In *Controlled Environment Horticulture: Improving Quality of Vegetables and Medicinal Plants*; Springer International Publishing: Cham, Switzerland, 2019; pp. 19–33.
9. Meyer, J.; Murray, S.L.; Berger, D.K. Signals that stop the rot: Regulation of secondary metabolite defences in cereals. *Physiol. Mol. Plant Pathol.* **2016**, *94*, 156–166. [CrossRef]
10. Zhao, N.; Wang, G.; Norris, A.; Chen, X.; Chen, F. Studying plant secondary metabolism in the age of genomics. *Crit. Rev. Plant Sci.* **2013**, *32*, 369–382. [CrossRef]
11. Hammerschmidt, R. Phytoalexins: What have we learned after 60 years? *Annu. Rev. Phytopathol.* **1999**, *37*, 285–306. [CrossRef]
12. Grayer, R.J.; Harborne, J.B. A survey of antifungal compounds from higher plants, 1982–1993. *Phytochemistry* **1994**, *37*, 19–42. [CrossRef]
13. Nicholson, R.L.; Hammerschmidt, R. Phenolic compounds and their role in disease resistance. *Annu. Rev. Phytopathol.* **1992**, *30*, 369–389. [CrossRef]
14. Shin, S.; Zheng, P.; Fazio, G.; Mazzola, M.; Main, D.; Zhu, Y. Transcriptome changes specifically associated with apple *(Malus domestica*) root defense response during *Pythium ultimum* infection. *Physiol. Mol. Plant Pathol.* **2016**, *94*, 16–26. [CrossRef]
15. Zhu, Y.; Saltzgiver, M.; Zhao, J. A phenotyping protocol for detailed evaluation of apple root resistance responses utilizing tissue culture micropropagated apple plants. *Am. J. Plant Sci.* **2018**, *9*, 2183. [CrossRef]
16. Zhu, Y.; Zhao, J.; Zhou, Z. Identifying an elite panel of apple rootstock germplasm with contrasting root resistance to *Pythium ultimum*. *J. Plant Pathol. Microbiol.* **2018**, *9*, 1000461. [CrossRef]
17. Zhu, Y.; Shao, J.; Zhou, Z.; Davis, R.E. Genotype-specific suppression of multiple defense pathways in apple root during infection by *Pythium ultimum*. *Hort. Res.* **2019**, *6*, 10. [CrossRef]
18. Zhu, Y.; Li, G.; Singh, J.; Khan, A.; Fazio, G.; Saltzgiver, M.; Xia, R. Laccase Directed Lignification Is One of the Major Processes Associated With the Defense Response Against *Pythium ultimum* Infection in Apple Roots. *Front. Plant Sci.* **2021**, *12*, 629776. [CrossRef]
19. Zhu, Y.; Zhou, Z. Challenges and Progress in Evaluating Apple Root Resistance Responses to *Pythium ultimum* Infection. *Am. J. Plant Sci.* **2023**, *14*, 1410–1429. [CrossRef]
20. Zhu, Y.; Shao, J.; Zhou, Z.; Davis, R.E. Comparative transcriptome analysis reveals a preformed defense system in apple root of a resistant genotype of G.935 in the absence of pathogen. *Int. J. Plant Genom.* **2017**, *2017*, 8950746. [CrossRef]
21. Zhu, Y.; Zhou, Z. The genotype-specific laccase gene expression and lignin deposition patterns in apple root during *Pythium ultimum* infection. *Fruit Res.* **2021**, *1*, 12. [CrossRef]
22. Upadhyay, N.; Kar, D.; Deepak Mahajan, B.; Nanda, S.; Rahiman, R.; Panchakshari, N.; Bhagavatula, L.; Datta, S. The multitasking abilities of MATE transporters in plants. *J. Exp. Bot.* **2019**, *70*, 4643–4656. [CrossRef] [PubMed]
23. Zhao, J. Flavonoid transport mechanisms: How to go, and with whom. *Trends Plant Sci.* **2015**, *20*, 576–585. [CrossRef] [PubMed]
24. Zhang, W.; Liao, L.; Xu, J.; Han, Y.; Li, L. Genome-wide identification, characterization and expression analysis of MATE family genes in apple (*Malus* × *domestica* Borkh). *BMC Genom.* **2021**, *22*, 632. [CrossRef] [PubMed]
25. Zhu, Y.; Shin, S.; Mazzola, M. Genotype responses of two apple rootstocks to infection by *Pythium ultimum* causing apple replant disease. *Can. J. Plant Pathol.* **2016**, *38*, 483–491. [CrossRef]
26. Livak, K.J.; Schmittgen, T.D. Analysis of relative gene expression data using real-time quantitative PCR and the $2^{-\Delta\Delta CT}$ method. *Methods* **2001**, *25*, 402–408. [CrossRef]
27. Langmead, B.; Salzberg, S.L. Fast gapped-read alignment with Bowtie 2. *Nat. Methods* **2012**, *9*, 357. [CrossRef]
28. Love, M.I.; Huber, W.; Anders, S. Moderated estimation of fold change and dispersion for RNA-seq data with DESeq2. *Genome Biol.* **2014**, *15*, 550. [CrossRef]
29. Altschul, S.F.; Gish, W.; Miller, W.; Myers, E.W.; Lipman, D.J. Basic local alignment search tool. *J. Mol. Biol.* **1990**, *215*, 403–410. [CrossRef]
30. Kolde, R. pheatmap: Pretty Heatmaps. 2019. Available online: https://CRAN.R-project.org/package=pheatmap (accessed on 8 August 2024).
31. Lescot, M.; Déhais, P.; Thijs, G.; Marchal, K.; Moreau, Y.; Van de Peer, Y.; Rouzé, P.; Rombauts, S. PlantCARE, a database of plant cis-acting regulatory elements and a portal to tools for in silico analysis of promoter sequences. *Nucleic Acids Res.* **2002**, *30*, 325–327. [CrossRef]

32. Chow, C.-N.; Yang, C.-W.; Wu, N.-Y.; Wang, H.-T.; Tseng, K.-C.; Chiu, Y.-H.; Lee, T.-Y.; Chang, W.-C. PlantPAN 4.0: Updated database for identifying conserved non-coding sequences and exploring dynamic transcriptional regulation in plant promoters. *Nucleic Acids Res.* **2024**, *52*, D1569–D1578. [CrossRef]
33. Chen, C.; Wu, Y.; Li, J.; Wang, X.; Zeng, Z.; Xu, J.; Liu, Y.; Feng, J.; Chen, H.; He, Y. TBtools-II: A "one for all, all for one" bioinformatics platform for biological big-data mining. *Mol. Plant* **2023**, *16*, 1733–1742. [CrossRef] [PubMed]
34. Zhou, Z.; Tian, Y.; Cong, P.; Zhu, Y. Functional characterization of an apple *(Malus* x *domestica*) LysM domain receptor encoding gene for its role in defense response. *Plant Sci.* **2018**, *269*, 56–65. [CrossRef] [PubMed]
35. Zhou, Z.; Zhu, Y.; Tian, Y.; Yao, J.-L.; Bian, S.; Zhang, H.; Zhang, R.; Gao, Q.; Yan, Z. MdPR4, a pathogenesis-related protein in apple, is involved in chitin recognition and resistance response to apple replant disease pathogens. *J. Plant Physiol.* **2021**, *260*, 153390. [CrossRef] [PubMed]
36. Zhu, Y. The Feasibility of Using Autofluorescence to Detect Lignin Deposition Pattern during Defense Response in Apple Roots to *Pythium ultimum* Infection. *Horticulturae* **2022**, *8*, 1085. [CrossRef]
37. Zhu, Y.; Jordan, R.; Zhou, Z. Microscopic features of lignin deposition patterns in young apple roots using brightfield and fluorescence imaging. *Fruit Res.* **2023**, *4*, e007. [CrossRef]
38. Eckardt, N.A. Move It on Out with MATEs. *Plant Cell* **2001**, *13*, 1477–1480. [CrossRef]
39. Takanashi, K.; Shitan, N.; Yazaki, K. The multidrug and toxic compound extrusion (MATE) family in plants. *Plant Biotechnol.* **2014**, *31*, 417–430. [CrossRef]
40. Birkenbihl, R.P.; Liu, S.; Somssich, I.E. Transcriptional events defining plant immune responses. *Curr. Opin. Plant Biol.* **2017**, *38*, 1–9. [CrossRef]
41. Chezem, W.R.; Clay, N.K. Regulation of plant secondary metabolism and associated specialized cell development by MYBs and bHLHs. *Phytochemistry* **2016**, *131*, 26–43. [CrossRef]
42. Moore, J.W.; Loake, G.J.; Spoel, S.H. Transcription Dynamics in Plant Immunity. *Plant Cell* **2011**, *23*, 2809–2820. [CrossRef]
43. Pireyre, M.; Burow, M. Regulation of MYB and bHLH Transcription Factors: A Glance at the Protein Level. *Mol. Plant* **2015**, *8*, 378–388. [CrossRef] [PubMed]
44. Xu, W.; Dubos, C.; Lepiniec, L. Transcriptional control of flavonoid biosynthesis by MYB–bHLH–WDR complexes. *Trends Plant Sci.* **2015**, *20*, 176–185. [CrossRef] [PubMed]
45. Bakshi, M.; Oelmüller, R. WRKY transcription factors: Jack of many trades in plants. *Plant Signal. Behav.* **2014**, *9*, e27700. [CrossRef] [PubMed]
46. Birkenbihl, R.P.; Diezel, C.; Somssich, I.E. Arabidopsis WRKY33 is a key transcriptional regulator of hormonal and metabolic responses toward Botrytis cinerea infection. *Plant Physiol.* **2012**, *159*, 266–285. [CrossRef] [PubMed]
47. Pandey, S.P.; Somssich, I.E. The role of WRKY transcription factors in plant immunity. *Plant Physiol.* **2009**, *150*, 1648–1655. [CrossRef]
48. Chen, X.; Li, S.; Zhang, D.; Han, M.; Jin, X.; Zhao, C.; Wang, S.; Xing, L.; Ma, J.; Ji, J. Sequencing of a wild apple (*Malus baccata*) genome unravels the differences between cultivated and wild apple species regarding disease resistance and cold tolerance. *G3 Genes Genomes Genet.* **2019**, *9*, 2051–2060. [CrossRef]
49. Daccord, N.; Celton, J.-M.; Linsmith, G.; Becker, C.; Choisne, N.; Schijlen, E.; Van de Geest, H.; Bianco, L.; Micheletti, D.; Velasco, R. High-quality de novo assembly of the apple genome and methylome dynamics of early fruit development. *Nat. Genet.* **2017**, *49*, 1099–1106. [CrossRef]
50. Li, Z.; Wang, L.; He, J.; Li, X.; Hou, N.; Guo, J.; Niu, C.; Li, C.; Liu, S.; Xu, J. Chromosome-scale reference genome provides insights into the genetic origin and grafting-mediated stress tolerance of Malus prunifolia. *Plant Biotechnol. J.* **2022**, *20*, 1015–1017. [CrossRef]
51. Velasco, R.; Zharkikh, A.; Affourtit, J.; Dhingra, A.; Cestaro, A.; Kalyanaraman, A.; Fontana, P.; Bhatnagar, S.K.; Troggio, M.; Pruss, D. The genome of the domesticated apple (*Malus* × *domestica* Borkh.). *Nat. Genet.* **2010**, *42*, 833. [CrossRef]
52. Zhang, L.; Hu, J.; Han, X.; Li, J.; Gao, Y.; Richards, C.M.; Zhang, C.; Tian, Y.; Liu, G.; Gul, H. A high-quality apple genome assembly reveals the association of a retrotransposon and red fruit colour. *Nat. Commun.* **2019**, *10*, 1494. [CrossRef]
53. Vance, C.; Kirk, T.; Sherwood, R. Lignification as a mechanism of disease resistance. *Annu. Rev. Phytopathol.* **1980**, *18*, 259–288. [CrossRef]
54. Vanholme, R.; Demedts, B.; Morreel, K.; Ralph, J.; Boerjan, W. Lignin biosynthesis and structure. *Plant Physiol.* **2010**, *153*, 895–905. [CrossRef] [PubMed]
55. Bhuiyan, N.H.; Selvaraj, G.; Wei, Y.; King, J. Role of lignification in plant defense. *Plant Signal. Behav.* **2009**, *4*, 158–159. [CrossRef] [PubMed]
56. Xu, L.; Zhu, L.; Tu, L.; Liu, L.; Yuan, D.; Jin, L.; Long, L.; Zhang, X. Lignin metabolism has a central role in the resistance of cotton to the wilt fungus Verticillium dahliae as revealed by RNA-Seq-dependent transcriptional analysis and histochemistry. *J. Exp. Bot.* **2011**, *62*, 5607–5621. [CrossRef]
57. Lee, M.H.; Jeon, H.S.; Kim, S.H.; Chung, J.H.; Roppolo, D.; Lee, H.J.; Cho, H.J.; Tobimatsu, Y.; Ralph, J.; Park, O.K. Lignin-based barrier restricts pathogens to the infection site and confers resistance in plants. *EMBO J.* **2019**, *38*, e101948. [CrossRef]

Disclaimer/Publisher's Note: The statements, opinions and data contained in all publications are solely those of the individual author(s) and contributor(s) and not of MDPI and/or the editor(s). MDPI and/or the editor(s) disclaim responsibility for any injury to people or property resulting from any ideas, methods, instructions or products referred to in the content.